

Elastic properties of three-dimensional Yukawa or dust crystals from molecular dynamic simulations

Sandeep Kumar^{1,*}

¹*Department of Physics, University of South Florida, Tampa, Florida 33620, USA*

(Dated: April 26, 2024)

I calculate elastic properties of three-dimensional Yukawa or dust crystals using molecular dynamic simulations. The elastic properties are computed by deforming (compressing/expanding) a cubic dust crystal along different directions. The bulk modulus, shear modulus, and Poisson's ratio are determined as a function of shielding parameter κ and strong coupling parameter Γ . Furthermore, I calculate sound wave velocity and shear wave velocity using bulk and shear modulus values and compare them with the velocities obtained from the slope of longitudinal and transverse wave dispersion relations. It is found that the sound and shear velocities obtained using bulk and shear modulus agree with the previously observed experimental values.

I. INTRODUCTION

Dusty plasmas are composed of electrons, ions, neutrals, and immersed dust particles. It is observed in both natural and laboratory settings. In nature, dusty plasmas are observed in Saturn's ring, interstellar clouds, and cometary tails [1]. In laboratory, it is present in the plasmas of fusion devices, rocket exhaust, and created in experimental devices under controlled conditions [2, 3]. The dusty plasma offers a model system to study generic phenomena such as self-organization and transport at particle level [4]. Both theoretical and experimental studies have been carried out to study generic phenomena in dusty plasmas, such as crystallization [5–7], single particle dynamics [8, 9], solitons [10–13], shocks [14, 15], spiral waves [16, 17], vortices [18, 19], and Mach cones [20].

A typical micron-sized dust particle carries an electronic charge ranging from approximately $-10,000e$ to $-20,000e$ and possesses a mass approximately 10^{13} to 10^{14} times that of ions. Dusty plasma can be modeled by a system of point particles interacting through a Yukawa potential, also known as a shielded Coulomb potential, described by the following expression [21]:

$$U(r) = \frac{Q^2}{4\pi\epsilon_0 r} \exp\left(-\frac{r}{\lambda_D}\right), \quad (1)$$

where $Q = -Z_d e$ is the charge on a typical dust particle, r is the separation between two dust particles, and λ_D is the Debye length of background plasma. The Yukawa system can be characterized in terms of two dimensionless parameters $\Gamma = Q^2/4\pi\epsilon_0 a k_B T_d$ (known as the strong coupling parameter) and $\kappa = a/\lambda_D$ (known as the shielding parameter). Here, T_d and a are the dust temperature and the Wigner-Seitz (WS) radius, respectively. The Yukawa inter-particle interaction is also used to model other systems, including charged colloids [22, 23], electrolytes [24, 25], and strongly coupled electron-ion plasmas [26, 27].

Elastic properties are crucial material characteristics that indicate the stiffness of a material. They are linked to the propagation of waves and their velocities along specific crystallographic directions within a material. Wave propagation and viscoelasticity in dusty plasmas have been extensively investigated through experiments and simulations over the past few decades [4]. Earlier studies have been carried out to calculate the elastic properties of Yukawa systems. Robbins *et al.* [28] and Khrapak and Klumov [29] have conducted simulations where sound velocities and radial distribution functions have been utilized in the calculations of elastic properties of Yukawa systems, respectively. Wang *et al.* [30] have determined the shear modulus of two-dimensional dusty plasmas by considering the viscoelasticity of the liquid state. More recently, Kozhberov [31] have studied the elastic properties of Yukawa crystals using analytical expressions, incorporating the electrostatic energies of deformed crystals in the calculations. The investigation into the elastic properties of Yukawa or dust crystals continues to be an area of sustained interest.

In this paper, I calculate the elastic properties of dusty plasma by deforming (compressing/expanding) a cubic dust crystal along different directions. The stress and strain of the deformed crystal are used in the calculation of the elastic stiffness constants of dusty plasma. Furthermore, these elastic constants are utilized to calculate the bulk modulus, shear modulus, and Poisson's ratio of the Yukawa crystal. I determine the bulk modulus, shear modulus, and Poisson's ratio as functions of the shielding parameter κ and the strong coupling parameter Γ . These elastic properties are calculated using experimental dusty plasma parameters. I assess the accuracy of my elastic property calculations by comparing the sound velocity and shear velocity obtained using it with those obtained from the slope of longitudinal and transverse wave dispersion relations.

The paper is organized as follows. Section II provides details of molecular dynamic (MD) simulations. In Section III, I report the results for elastic properties as a function of strong coupling parameter Γ and shielding parameter κ . Section IV contains a summary of the work.

* sandeepshukla1112@gmail.com/sandeepk15@usf.edu

II. SIMULATION METHOD

A three-dimensional cubic box containing point particles is created to study the elastic properties of dust crystals. Yukawa interaction potential is taken among the dust particles, which mimics the screening from background electrons and ions. The state-of-the-art open-source code LAMMPS [32] is used for the molecular dynamic simulations. The simulation box contains 10235 dust particles within dimensions of $35a \times 35a \times 35a$ (ranging from 0 to $35a$) along the X, Y, and Z directions, respectively, where a is average inter-particle distance. Experimental parameters [18] are employed in the simulations: $Q = -20000e$ (where e denotes the charge of an electron), dust mass $m = 1.7 \times 10^{-13}$ Kg, and average inter-particle distance $a = 6 \times 10^{-4}$ m. The average inter-particle distance sets the number density of dust particles $n = 1.1 \times 10^9$ per m^3 , corresponding to a mass density ρ of 1.87×10^{-4} Kg/ m^3 . In the simulations, the value of shielding parameter κ is increased by decreasing the screening length λ_D of the Yukawa interaction, and the value of strong coupling parameter Γ is increased by decreasing the temperature of dust particles.

The particles are equilibrated at a given temperature using Langevin dynamics, which reads as

$$m\ddot{\mathbf{r}}_i = - \sum_j \nabla U_{ij} + \mathbf{F}_f + \mathbf{F}_r, \quad (2)$$

where U_{ij} is interaction potential, \mathbf{F}_f is frictional force on the particles, and \mathbf{F}_r is random force (kicks) on the particles. I choose simulation time step of 100 μs , which ensures a fine discretization along the temporal domain and good resolution of the underlying dust kinetics. The dust particles are evolved for the 40000 time steps for the equilibration of the system. Fluctuations in temperature, pressure, and total energy of the system over time are monitored to verify system equilibration.

Following equilibration, the system is prepared for the calculation of elastic properties under isothermal conditions. The cubic box is transformed into a triclinic box and equilibrated again for 450000 time steps. Subsequently, the triclinic box undergoes deformation (Voigt deformation) along various directions. After each expansion and contraction, the triclinic box is equilibrated for 50000 time steps. The change in the stress of crystal P_x , P_y , P_z , P_{xy} , P_{xz} , P_{yz} with deformation (strain) along X, Y, Z, XY, XZ, and YZ directions (Voigt deformation component), respectively, are used in the calculations of elastic stiffness constants.

The convergence of elastic properties with magnitude of deformation (expansion/compression) is checked carefully. A deformation magnitude of 0.075 (in strain units) is employed in my calculations. The average of stresses are taken at 1000 time steps. The finite size effects on elastic properties are examined, which reveals that 10235 atoms are adequate to mitigate such effects.

III. RESULTS

The purpose of this study is to calculate elastic properties of three-dimensional Yukawa or dust crystal as a function of κ and Γ . Specifically, I compute the bulk modulus, shear modulus, and Poisson's ratio to characterize the elastic properties.

A. Bulk Modulus

The bulk modulus K is a measure of the resistance of a material to an applied bulk compression. I calculate bulk modulus using the following expression [28, 33]:

$$K = \frac{C_{11} + 2C_{12}}{3}. \quad (3)$$

In the above expression, C_{11} and C_{12} are the elastic stiffness constants. The bulk modulus at $\Gamma = 2000$ as a function of screening parameter κ is displayed in Fig. 1. It decreases with an increase in the κ . This reduction occurs because as κ increases, the interaction potential length decreases, making compression of the material easier. For large κ , the Yukawa potential becomes extremely short-range, leading to interactions among particles resembling those in a hard sphere system. The characteristics of bulk modulus at $\kappa = 2$ with varying strong coupling parameter Γ is shown in Fig. 2. The bulk modulus decreases with an increase in Γ . In this study, Γ is increased by reducing the temperature of the dust particles, making it easier to compress the particles due to reduced thermal pressure. However, at higher Γ values, the rigidity driven by the interaction potential overtakes the rigidity driven by temperature, resulting in no further change in bulk modulus with decreasing temperature (see Fig. 2).

To validate the accuracy of my bulk modulus calculations, I compute the longitudinal sound velocity C_S using it. I utilize the relationship $C_S = \sqrt{K/\rho}$ for the calculation of sound velocity [33]. At $\kappa = 2.0$ and $\Gamma = 3000$, the sound velocity obtained using bulk modulus is 2.01 cm/s, which closely matches the sound velocity value of 2.15 cm/s obtained from the slope of the longitudinal wave dispersion relation, see Fig. S1 in supplementary material. The details of the sound velocity calculation from the dispersion relation are provided in the supplementary material [34] and have also been recently reported by Kumar *et al.* [35]. The experimentally measured and theoretically calculated values of sound velocity by Bailung *et al.* [18] at the same parameters are 4.5 cm/s and 3.06 cm/s, respectively. From these comparisons, it is evident that my bulk modulus values yield correct sound velocity in the dusty plasma medium. The strongly coupled dusty plasmas are extremely soft, so that the bulk modulus of solid dusty plasma is much smaller than those of typical solids like metals. For example, bulk modulus of aluminum at ambient condition is 79 GPa [36].

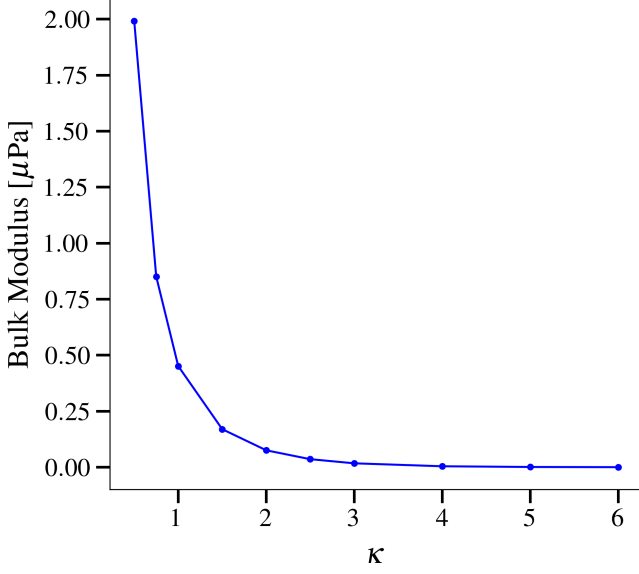


FIG. 1. Bulk modulus K of dust crystal at the strong coupling parameter $\Gamma = 2000$ as a function of shielding parameter κ .

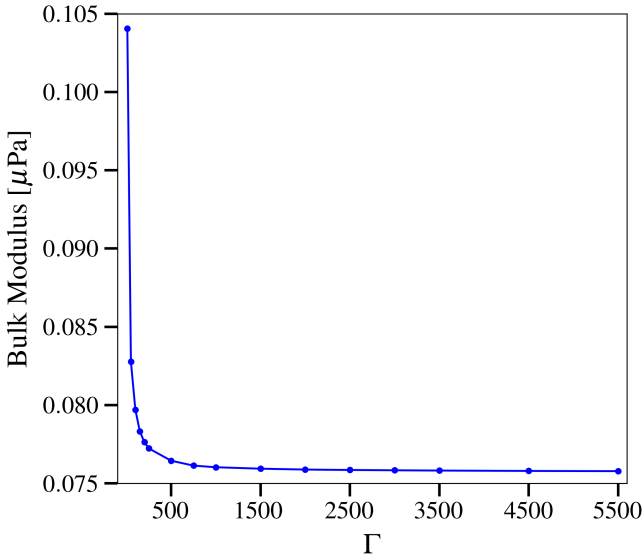


FIG. 2. Bulk modulus K of dust crystal at shielding parameter $\kappa = 2$ as a function of strong coupling parameter Γ .

B. Shear Modulus

The shear modulus G is a measure of a material's resistance to an applied shearing deformation. I calculate the shear modulus using the following formulas [28, 33]:

$$G_1 = C_{44} \quad (4)$$

and

$$G_2 = \frac{C_{11} - C_{12}}{2}. \quad (5)$$

Here, G_1 and G_2 are the shear modulus along 100 and 110 crystallographic directions, respectively. The shear modulus G_1 as a function of Γ at different κ values is displayed in Fig. 3. Additionally, the shear modulus as a function of κ at $\Gamma = 2000$ along the 100 and 110 crystallographic directions are shown in Fig. 4. The values of G_1 and G_2 differ at small κ values because the particles are in a crystalline phase, resulting in different particle arrangements along the 100 and 110 directions, leading to different shear strains along these directions. However, at high κ values, the particles are in a liquid phase and exhibit a uniform distribution along all directions resulting in G_1 and G_2 are equal. In the crystalline phase, the shear modulus decreases with an increase in the shielding parameter, which is a direct consequence of the reduction in inter-particle interactions. The shear modulus initially decreases with an increase in the strong coupling parameter Γ , and later it increases with further increases in the strong coupling parameter due to an increase in inter-particle interactions. This increase in inter-particle interaction results in an increase in resistance to an applied shear deformation. At very high Γ values, temperature-driven shear deformation becomes very low and is suppressed by inter-particle driven shear resistance, consequently causing the shear modulus to saturate (see Fig. 3).

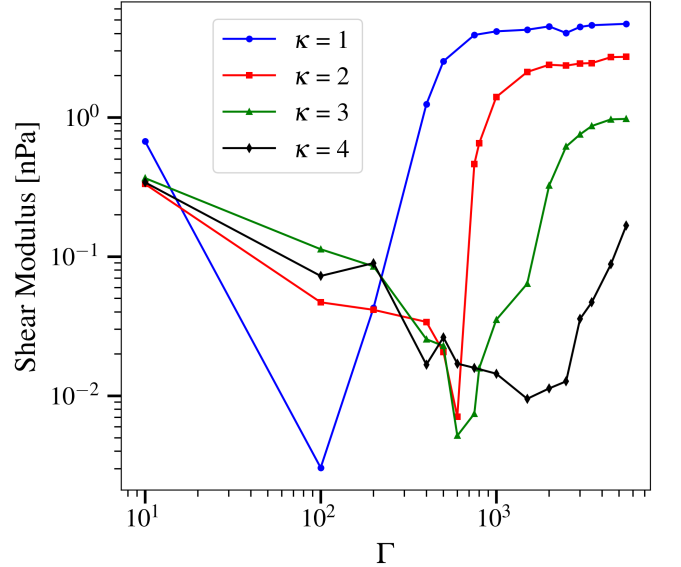


FIG. 3. Shear modulus G_1 of dust crystal at different shielding parameters κ as a function of strong coupling parameter Γ .

At $\kappa = 2.0$ and $\Gamma = 3000$, the shear velocity obtained from the shear modulus relation $C_T = \sqrt{G/\rho}$ [33] is 3.61 mm/s and 3.59 mm/s along the 100 and 110 directions, respectively. These values are close to the experimentally measured value of 4.2 mm/s reported by Pramanik *et al.* [37]. Nunomura *et al.* [38] have also reported similar values of shear velocity in their experiments. From the slope

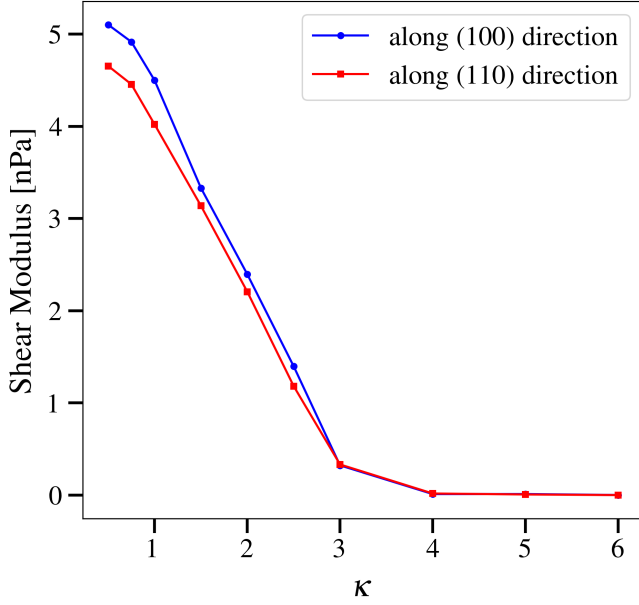


FIG. 4. Shear modulus of dust crystal along crystallographic directions of 100 and 110 as a function of shielding parameter κ . The strong coupling parameter Γ of the Yukawa crystal is 2000.

of the transverse wave dispersion relation, the obtained shear velocity is 5.36 mm/s, see Fig. S2 in the supplementary material [34]. Nevertheless, my shear modulus values are providing correct shear velocity in the dusty plasma medium. Similar to the bulk modulus, the shear modulus is much smaller than that of typical solids. For instance, the shear modulus for aluminum at ambient conditions is 25.5 GPa [39].

C. Poisson's Ratio

The Poisson's ratio ν quantifies the deformation (compression/expansion) of a material in directions perpendicular to a specific direction of loading. It is defined as the negative ratio of transverse strain to axial strain. I calculate Poisson's ratio using the elastic constants, which is given by

$$\nu = \frac{1}{1 + \frac{C_{11}}{C_{12}}}. \quad (6)$$

The Poisson's ratio at $\Gamma = 2000$ as a function of κ is displayed in Fig. 5. Initially, Poisson's ratio decreases with an increase in κ because transverse strain decreases with the reduction in interaction length of potential. However, above $\kappa > 2.5$, it increases because the Yukawa interaction becomes extremely short-range, resulting in interactions among particles resembling those in a hard sphere system that leads to much less axial strain. The characteristics of Poisson's ratio at $\kappa = 2$ as a function of Γ is shown in Fig. 6. With an increase in the strong

coupling parameter Γ , Poisson's ratio decreases, which is a direct consequence of less strain in the transverse direction due to the reduced thermal motion (thermal pressure) of particles at low temperatures.

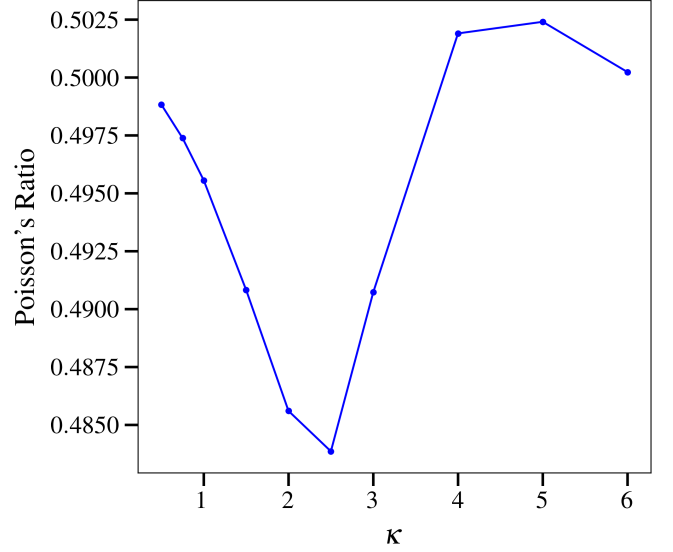


FIG. 5. Poisson's ratio of dust crystal at coupling parameter $\Gamma = 2000$ as a function of shielding parameter κ .

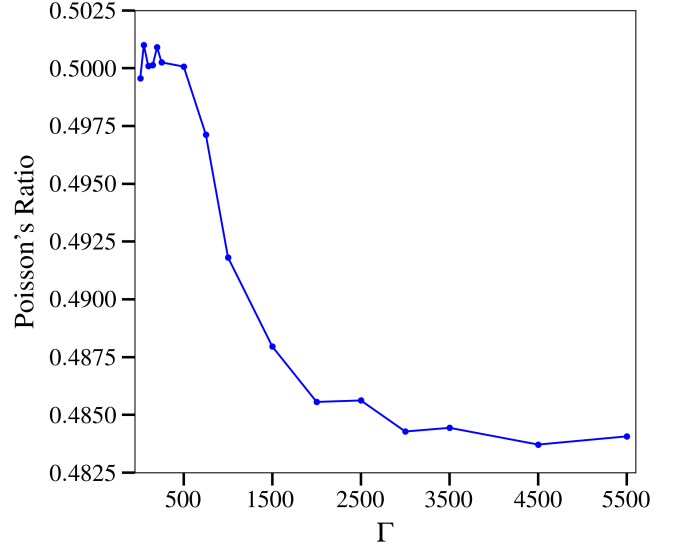


FIG. 6. Poisson's ratio of dust crystal at shielding parameter $\kappa = 2$ as a function of coupling parameter Γ .

For dusty plasma, the bulk modulus is much larger compared to the shear modulus, so they can be regarded as effectively incompressible, as it is easier to change shape than to compress. Soft materials with similar characteristics are also considered incompressible in nature [40]. A perfectly incompressible isotropic material has a Poisson's ratio of exactly 0.5; for dusty plasma, it

is approximately 0.5. However, the incompressible nature of dusty plasma changes with variations in κ and Γ , see Fig. 5 and Fig. 6. For comparison, it is worth mentioning that the Poisson's ratio of natural rubber and aluminum is 0.4999 and 0.33, respectively [41].

IV. SUMMARY

I have calculated bulk modulus, shear modulus, and Poisson's ratio of a cubic Yukawa or dusty crystal in the molecular dynamic simulations. These properties are computed by deforming (compressing/expanding) the dust crystal along different directions. The characteristics of elastic properties as a function of shielding parameter and strong coupling parameter have been studied. The shear modulus has also been calculated along the crystallographic directions of 100 and 110, and it is found that the values are different at small screening parameters. Furthermore, I have calculated sound and shear wave velocities using bulk and shear modulus and compared them with the velocities obtained from the slope of longitudinal and transverse wave dispersion relations.

It is found that the sound and shear velocities obtained using bulk and shear modulus agree with the previously observed experimental values.

Strongly coupled dusty plasmas exhibit solid-like traits, but they are extremely soft. As a result, the bulk modulus and shear modulus of solid dusty plasmas are much smaller than those of typical solids, such as metals. In fact, the bulk modulus is much larger compared to the shear modulus, which effectively renders dusty plasma as incompressible. This is because it is easier to change shape than to compress a dusty plasma system.

ACKNOWLEDGMENTS

The author thanks Dr. Attila Cangi (CASUS-HZDR, Görlitz, Germany) and Dr. Svetoslav Nikolov (SNL, Albuquerque, USA) for helpful discussions. The computations were performed on a Bull Cluster at the Center for Information Services and High Performance Computing (ZIH) at Technische Universität Dresden, on the cluster Hemera at Helmholtz-Zentrum Dresden-Rossendorf (HZDR).

-
- [1] Padma K Shukla and AA Mamun, *Introduction to dusty plasma physics* (CRC press, 2015).
 - [2] JH Chu and I Lin, "Direct observation of coulomb crystals and liquids in strongly coupled rf dusty plasmas," *Phys. Rev. Lett.* **72**, 4009 (1994).
 - [3] Neeraj Chaubey and J Goree, "Coulomb expansion of a thin dust cloud observed experimentally under afterglow plasma conditions," *Phys. Plasmas* **29** (2022).
 - [4] Gregor E Morfill and Alexei V Ivlev, "Complex plasmas: An interdisciplinary research field," *Rev. Mod. Phys.* **81**, 1353 (2009).
 - [5] H. Thomas, G. E. Morfill, V. Demmel, J. Goree, B. Feuerbacher, and D. Möhlmann, "Plasma crystal: Coulomb crystallization in a dusty plasma," *Phys. Rev. Lett.* **73**, 652-655 (1994).
 - [6] S Hamaguchi, RT Farouki, and DHE Dubin, "Triple point of yukawa systems," *Phys. Rev. E* **56**, 4671 (1997).
 - [7] Srimanta Maity and Amita Das, "Molecular dynamics study of crystal formation and structural phase transition in yukawa system for dusty plasma medium," *Phys. Plasmas* **26** (2019).
 - [8] Srimanta Maity, Amita Das, Sandeep Kumar, and Sanat Kumar Tiwari, "Interplay of single particle and collective response in molecular dynamics simulation of dusty plasma system," *Phys. Plasmas* **25** (2018).
 - [9] Priya Deshwal, Mamta Yadav, Chaitanya Prasad, Shantam Sridev, Yash Ahuja, Srimanta Maity, and Amita Das, "Chaotic dynamics of small-sized charged yukawa dust clusters," *Chaos* **32** (2022).
 - [10] Sandeep Kumar, Sanat Kumar Tiwari, and Amita Das, "Observation of the korteweg-de vries soliton in molecular dynamics simulations of a dusty plasma medium," *Phys. Plasmas* **24**, 033711 (2017).
 - [11] P Bandyopadhyay, G Prasad, A Sen, and PK Kaw, "Experimental study of nonlinear dust acoustic solitary waves in a dusty plasma," *Phys. Rev. Lett.* **101**, 065006 (2008).
 - [12] Zoltán Donkó, Peter Hartmann, Ranna U Masheyeva, and Karlygash N Dzhumagulova, "Molecular dynamics investigation of soliton propagation in a two-dimensional yukawa liquid," *Contrib. Plasma Phys.* **60**, e201900197 (2020).
 - [13] Prince Kumar and Devendra Sharma, "Quasi-localized charge approximation approach for the nonlinear structures in strongly coupled yukawa systems," *Phys. Plasmas* **30** (2023).
 - [14] Sumita K Sharma, A Boruah, Y Nakamura, and H Bailung, "Observation of dust acoustic shock wave in a strongly coupled dusty plasma," *Phys. Plasmas* **23** (2016).
 - [15] Garima Arora and Srimanta Maity, "Self-excited converging shock structure in a complex plasma medium," *Phys. Rev. E* **108**, 055209 (2023).
 - [16] Sandeep Kumar, Bhavesh Patel, and Amita Das, "Spiral waves in driven dusty plasma medium: Generalized hydrodynamic fluid description," *Phys. Plasmas* **25**, 043701 (2018).
 - [17] Sandeep Kumar and Amita Das, "Spiral waves in driven strongly coupled yukawa systems," *Phys. Rev. E* **97**, 063202 (2018).
 - [18] Yoshiko Bailung, Bidyut Chutia, T Deka, A Boruah, Sumita K Sharma, Sandeep Kumar, Joyanti Chutia, Y Nakamura, and H Bailung, "Vortex formation in a strongly coupled dusty plasma flow past an obstacle," *Phys. Plasmas* **27** (2020).
 - [19] Vikram S Dharodi, "Rotating vortices in two-dimensional inhomogeneous strongly coupled dusty plasmas: Shear and spiral density waves," *Phys. Rev. E* **102**, 043216 (2020).

- (2020).
- [20] D Samsonov, J Goree, ZW Ma, A Bhattacharjee, HM Thomas, and GE Morfill, “Mach cones in a coulomb lattice and a dusty plasma,” *Phys. Rev. Lett.* **83**, 3649 (1999).
 - [21] U. Konopka, G. E. Morfill, and L. Ratke, “Measurement of the interaction potential of microspheres in the sheath of a rf discharge,” *Phys. Rev. Lett.* **84**, 891–894 (2000).
 - [22] T. Palberg, W. Mönch, F. Bitzer, R. Piazza, and T. Bellini, “Freezing transition for colloids with adjustable charge: A test of charge renormalization,” *Phys. Rev. Lett.* **74**, 4555–4558 (1995).
 - [23] Takamichi Terao and Tsuneyoshi Nakayama, “Crystallization in quasi-two-dimensional colloidal systems at an air-water interface,” *Phys. Rev. E* **60**, 7157–7162 (1999).
 - [24] Yan Levin, “Electrostatic correlations: from plasma to biology,” *Rep. Prog. Phys.* **65**, 1577 (2002).
 - [25] Alpha A. Lee, Carla S. Perez-Martinez, Alexander M. Smith, and Susan Perkin, “Scaling analysis of the screening length in concentrated electrolytes,” *Phys. Rev. Lett.* **119**, 026002 (2017).
 - [26] M. Lyon, S. D. Bergeson, and M. S. Murillo, “Limit of strong ion coupling due to electron shielding,” *Phys. Rev. E* **87**, 033101 (2013).
 - [27] Jan Vorberger, Z Donko, IM Tkachenko, and Dirk O Gericke, “Dynamic ion structure factor of warm dense matter,” *Phys. Rev. Lett.* **109**, 225001 (2012).
 - [28] Mark O Robbins, Kurt Kremer, and Gary S Grest, “Phase diagram and dynamics of yukawa systems,” *J. Chem. Phys.* **88**, 3286–3312 (1988).
 - [29] Sergey A Khrapak and Boris A Klumov, “Instantaneous shear modulus of yukawa fluids across coupling regimes,” *Phys. Plasmas* **27** (2020).
 - [30] Kang Wang, Dong Huang, and Yan Feng, “Shear modulus of two-dimensional yukawa or dusty-plasma solids obtained from the viscoelasticity in the liquid state,” *Phys. Rev. E* **99**, 063206 (2019).
 - [31] AA Kozhberov, “Elastic properties of yukawa crystals,” *Phys. Plasmas* **29** (2022).
 - [32] Aidan P Thompson, H Metin Aktulga, Richard Berger, Dan S Bolintineanu, W Michael Brown, Paul S Crozier, Pieter J In’t Veld, Axel Kohlmeyer, Stan G Moore, Trung Dac Nguyen, *et al.*, “Lammps-a flexible simulation tool for particle-based materials modeling at the atomic, meso, and continuum scales,” *Comput. Phys. Commun.* **271**, 108171 (2022).
 - [33] Charles Kittel and Paul McEuen, *Introduction to solid state physics* (John Wiley & Sons, 2018).
 - [34] See Supplemental Material at [URL will be inserted by publisher].
 - [35] Sandeep Kumar, Hossein Tahmasbi, Kushal Ramakrishna, Mani Lokamani, Svetoslav Nikolov, Julien Tranchida, Mitchell A. Wood, and Attila Cangi, “Transferable interatomic potential for aluminum from ambient conditions to warm dense matter,” *Phys. Rev. Res.* **5**, 033162 (2023).
 - [36] Gene Simmons, “Single crystal elastic constants and calculated aggregate properties,” *J. Grad. Res.* **34**, 1 (1965).
 - [37] J Pramanik, G Prasad, A Sen, and PK Kaw, “Experimental observations of transverse shear waves in strongly coupled dusty plasmas,” *Phys. Rev. Lett.* **88**, 175001 (2002).
 - [38] S Nunomura, D Samsonov, and J Goree, “Transverse waves in a two-dimensional screened-coulomb crystal (dusty plasma),” *Phys. Rev. Lett.* **84**, 5141 (2000).
 - [39] Robert R. Archer, Stephen H. Crandall, Norman C. Dahl, and Thomas J. Lardner, *An introduction to the mechanics of solids*, 2nd ed. (McGraw-Hill Kogakusha, 1972).
 - [40] Zbigniew D Jastrzebski, *Nature and properties of engineering materials* (John Wiley and Sons, Inc., New York, 1976).
 - [41] PH Mott and CM Roland, “Limits to poisson’s ratio in isotropic materials,” *Phys. Rev. B* **80**, 132104 (2009).

Supporting Information:

Elastic properties of three-dimensional
Yukawa or dust crystals from molecular
dynamic simulations

Sandeep Kumar*

Department of Physics, University of South Florida, Tampa, Florida 33620, USA

E-mail: sandeepshukla1112@gmail.com/sandeepk15@usf.edu

Contents

1 Longitudinal and Transverse Wave Velocity

S2

1 Longitudinal and Transverse Wave Velocity

The longitudinal sound wave velocity and transverse shear wave velocity of a material can be determined from the slope of the dispersion relation $\omega(\mathbf{q})$ at small \mathbf{q} values. The longitudinal $\lambda(\mathbf{q}, t)$ and transverse $\pi(\mathbf{q}, t)$ currents of dust particles are defined as

$$\lambda(\mathbf{q}, t) = \sum_j v_{jx}(t) e^{i\mathbf{q} \cdot \mathbf{x}_j(t)} \quad (1)$$

and

$$\pi(\mathbf{q}, t) = \sum_j v_{jy}(t) e^{i\mathbf{q} \cdot \mathbf{x}_j(t)} . \quad (2)$$

Here, \mathbf{x}_j , v_{jx} , and v_{jy} are the position, velocity in the X-direction, and velocity in the Y-direction of the j -th particle, respectively. The wave vector \mathbf{q} depends on the simulation system length L_x . The longitudinal and transverse current correlation spectrum

$$L(\mathbf{q}, \omega) = \frac{1}{2\pi N} \lim_{\tau \rightarrow \infty} \frac{1}{\tau} |\lambda(\mathbf{q}, \omega)|^2 \quad (3)$$

and

$$T(\mathbf{q}, \omega) = \frac{1}{2\pi N} \lim_{\tau \rightarrow \infty} \frac{1}{\tau} |\pi(\mathbf{q}, \omega)|^2 , \quad (4)$$

respectively, are calculated from the longitudinal $\lambda(\mathbf{q}, \omega)$ and transverse $\pi(\mathbf{q}, \omega)$ current spectrum that are Fourier transform of longitudinal and transverse current

$$\lambda(\mathbf{q}, \omega) = \int_0^\tau \lambda(\mathbf{q}, t) e^{-i\omega t} dt \quad (5)$$

and

$$\pi(\mathbf{q}, \omega) = \int_0^\tau \pi(\mathbf{q}, t) e^{-i\omega t} dt. \quad (6)$$

In the above expression, N and τ are the number of dust particles and simulation time, respectively. The peak position in $L(\mathbf{q}, \omega)$ and $T(\mathbf{q}, \omega)$ provides ω value for the given wave vector q value. The peak in the $L(\mathbf{q}, \omega)$ and $T(\mathbf{q}, \omega)$ indicates the maximum energy of the longitudinal and transverse collective modes, respectively. The ω versus q plot gives the longitudinal and transverse wave dispersion relations, which are displayed in Fig. S1 and Fig. S2, respectively. The slope of plot at small q values provides the longitudinal sound and transverse shear wave velocity in the Yukawa system or dusty plasma. The obtained values of sound wave velocity and shear wave velocity at $\Gamma = 3000$ and $\kappa = 2$ are 2.15 cm/s and 5.36 mm/s, respectively.

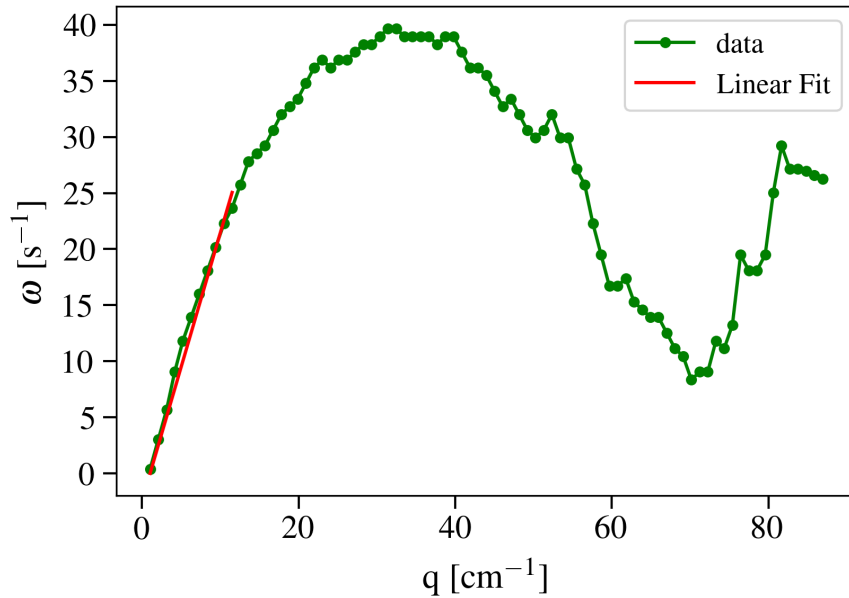


Figure S1: Longitudinal sound wave dispersion relation at the strong coupling parameter $\Gamma = 3000$ and shielding parameter $\kappa = 2$. The slope of plot at small q values (red line) provides sound wave velocity in the dusty plasma.

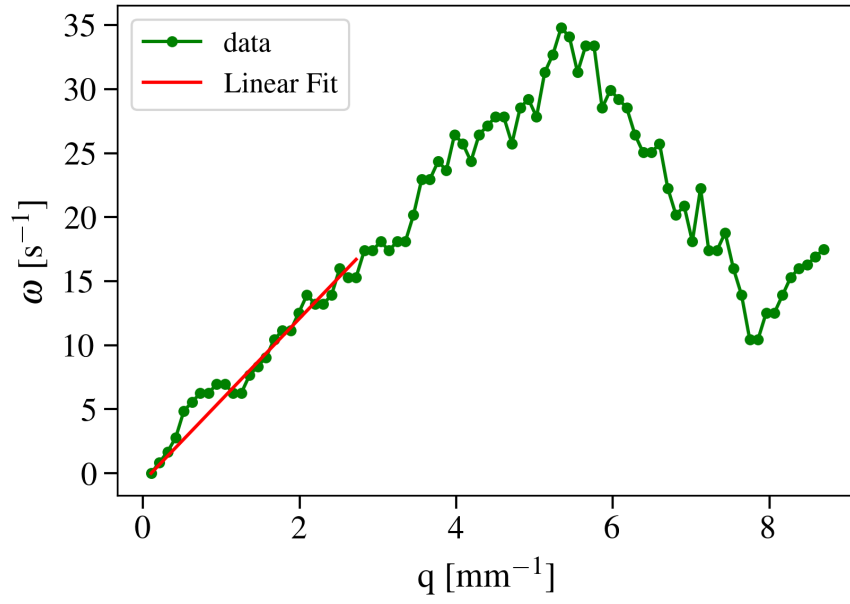


Figure S2: Transverse shear wave dispersion relation at the strong coupling parameter $\Gamma = 3000$ and shielding parameter $\kappa = 2$. The slope of plot at small q values (red line) provides shear wave velocity in the dusty plasma.